Hydration Heat and Shrinkage of the Support of High-performance Concrete-filled Steel Tubes

Huibin Sun[a], Xiao Zhang[b,*], Leisheng Zhou[c], Xing Shao[d]

[a]Research Center of Geotechnical and Structural Engineering,Shandong University, Jinan 250061, China
[b]School of Civil Engineering, Shandong University, Jinan 250061, China
[c]Shandong Provincial Communications Planning and Design Institute, Jinan 250031, China
[d]Qilu Transportation Development Group, Jinan 250101, China
xiaozhang3748@21cn.com

To strengthen the prevention of cracks in hydration heat engineering. On the basis of summarizing and analyzing the models for hydration heat of concrete, numerical methods are used to calculate the temperature change curve of the core concrete in cement hydration stage. The thermal performance parameters of steel tubes and concrete are the essential basic data, which serves as a basis for research. Sectional dimension largely influences the shrinkage distortion of the core concrete in the concrete-filled steel tubes, which increases as the dimensions of the cross-section expand.

1. Introduction

The support of high-performance concrete-filled steel tubes (CFST) is a common form of support in modern civil engineering, which mainly supports similar slopes and other structures through the combination of steel tubes and concrete. On the one hand, the stability of construction is improved, and on the other hand, the safety of construction workers is guaranteed. However, in the support structure of high-performance CFST, due to the concrete involved, the phenomenon of hydration heat may occur under the influence of temperature-related factors. The heat of hydration emerges mainly because concrete begins to emit a substantial amount of heat after being affected by temperature. As a result, there might be temperature differences between the inside and outside of concrete during the initial stage of solidification. If not processed in time, hydration heat would cause cracks in the concrete structure, thus affecting the overall structure of the support of high-performance CFST.

In order to strengthen the prevention of cracks caused by hydration heat engineering, this paper summarizes and analyzes the concrete hydration heat, shrinkage, creep models and corresponding calculation methods, applies numerical methods to calculate the temperature change curve and the shrinkage distortion curve of core concrete in the stage pf cement hydration as well as the creep deformation curve of the axially loaded and eccentrically loaded CFST under the long-term loading, and discusses the heat hydration, shrinkage and creep models for core concrete, hoping to provide reference for the CFST engineering practice.

2. Literature review

High flow self-compacting concrete (called high performance concrete) can be self-compacted under the condition of self-weight or less vibration. The filling of high performance concrete in steel pipe can not only guarantee the compactness of concrete better, but also simplify the vibration process of concrete, reduce the construction strength and cost of concrete, and reduce the noise pollution of the city. Self-compacting concrete was used in the top part of the Shenzhen SEG Plaza building built in 1999, and achieved good results. In the past twenty years, many domestic and foreign scholars have done a lot of experimental research and in-depth theoretical analysis on the deformation of concrete filled steel tube specimens under the long-term load, and have a certain understanding of the law and calculation method of the shrinkage and deformation development of the concrete filled steel tube components.

Based on the results of large test, elastoplastic dynamic analysis and parametric bending moment curvature analysis, the seismic performance of reinforced concrete filled steel tubular column / column pier is studied by Montejo. The results show that when the pile / column are curved with hyperbolic ratio, the ultimate state of the damage is largely controlled by the tensile strain of the top hinged steel longitudinal bar. When the pile / column are flexed by the single curvature, the limit state is controlled by the tensile strain of the steel pipe in the underground hinge. For single curvature bending and relatively thick steel pipes, Montejo also found that piles / columns may remain elastic in seismic events (Montejo, 2012). Kang et al. studied the axial compression strength of the steel tube high strength concrete composite column. The study obtained the peak value of axial direction and axial compression at the same time in the axial direction and axial compression of the concrete and reinforced concrete. After the damage to the reinforced concrete, the concrete filled steel tube can still bear the axial load and deformability, and the bearing capacity of the axial compression bearing capacity is affected. The main factors for axial bearing capacity are the constraint index, the strength of the outer concrete and the hoop characteristic value of the steel pipe (Kang et al., 2012). Lu et al. discussed the mechanical behavior of stress performance of confined concrete filled steel tube CFST columns confined with fiber reinforced polymer (FRP). Eleven columns were tested, and the effects of FRP number, thickness of steel pipe and concrete strength on the bearing capacity and axial deformation capacity were studied. The results show that FRP winding can effectively limit the expansion of concrete filled steel tubes and delay the local buckling of steel tubes. Under the constraint of FRP, the bearing capacity and axial deformation capacity of CFST columns can be greatly improved (Lu et al., 2014). Cao and others, through a long term creep test for more than 800 days in the indoor environment and the history of shrinkage and creep between different types of cylinders, including concrete columns, concrete-filled steel tubes and expansive concrete filled steel tubes, obtained the creep properties of shrinkage and steel tube expansive concrete. The results show that the shrinkage deformation of the steel tube expansive concrete is small, and the early shrinkage deformation is almost zero. Due to the influence of expansive agent, the creep deformation of steel tube expansive concrete varies greatly.

Based on the hypothesis that the creep mechanism of steel tube expansive concrete is reasonable, the estimation method of final creep coefficient of steel tube expansive concrete is proposed (Cao et al., 2015). Yuan and others discussed the behavior of pcfst pier under biaxial earthquake. Through a series of cyclic static load tests and single and bi-directional mixing (quasi dynamic) load tests, three different concrete proportions of circular cross-section specimens are studied. The results show that the restoring force of pcfst pier in bi-directional loading test is almost the same as that in unidirectional loading test, and the seismic performance of pcfst pier increases significantly with the height of concrete filling (Yuan et al., 2014). In order to prepare steel fiber reinforced micro expansive concrete with good fluidity, high anti segregation and good self-compacting, Zhou and others carried out compression test, splitting tensile test and bending test. The deformation behavior of steel fiber reinforced micro expansive concrete in steel tube was evaluated by self-developed concrete-filled steel tube expansion tester. Through 12 short column specimens, the structural behavior of steel fiber reinforced micro expansion concrete filled steel tube was studied. The invariants of expansive agent and the content of steel fiber are the main variables. The results show that the splitting tensile strength of SREC increases by 78% and 64.7%, respectively compared with that of conventional micro expansion concrete. When the dosage of expansive agent is 40Kg and the volume fraction of steel fiber is less than 1%, SECFST exhibits stable swelling deformation. The combination of steel fiber and expansive agent can increase the yield load and ultimate bearing capacity of concrete filled steel tube moderately (Zhou, et al., 2012).

Krishan and others carried out experimental and theoretical research on a new concrete filled steel tubular column. The design improvement idea is to make concrete filled steel tube columns with preloaded concrete core. The bearing capacity of the concrete filled steel tube axle center compression test specimen is increased by 20 to 25%. In this preliminary compressed CFST sample, the strength of the concrete core increases significantly, which is due to the three effects, the long-term compression of the concrete mixture, the initial lateral compression of the concrete core and the performance of the concrete core at the same time (Krishan et al., 2016). Huang et al. studied the structural damage assessment model of recycled concrete filled steel tubular structures under earthquake. The model takes into account the effects of lateral deformation and repeated cyclic loading. The available test results are collected and used to calibrate the parameters of the proposed model. The study shows that the seismic performance of RCFST components depends on the content of RCA, the damage index increases with the increase of the substitution rate of RCA, and the damage degree of RCFST varies with the change of the rate of RCA replacement. Finally, the RCA content, lateral deformation rate and damage degree are compared. An improved procedure is recommended to compensate for the performance difference between RCFST and ordinary concrete filled steel tube (CFST) (Huang et al., 2016).

In the early 1990s, domestic researchers first studied the stress redistribution of concrete filled steel tube arch bridges caused by creep. Since then, with the extensive application of the concrete filled steel tube arch bridge, people have paid more attention to the performance of the concrete filled steel tube and the system under the long-term load. The domestic researchers have carried out a lot of theoretical analysis and part of the experimental research, and some useful conclusions have been obtained. The recent research results in China show that the mechanical performance of the steel tube high performance concrete bending member is similar to that of the steel tube ordinary concrete. The calculation of the bearing capacity of the steel tube is basically based on the method of the ordinary concrete member of the steel tube. However, the research on hydration heat and shrinkage characteristics of high performance concrete pipe support at home and abroad is rarely reported. The characteristics of the hydration heat and shrinkage of the concrete filled steel tube reinforced concrete filled steel tube are studied. These are also the hot issues concerned by the engineering circles at present.

3. Methods

3.1 Production of samples

This experiment is conducted on two groups of samples: circular CFST and square CFST. Each group consists of two samples with the section dimensions of 200 mm and 1000 mm. The specific parameters of the test samples are indicated in Table 1, in which D(B) is the outer diameter of the section of the components (outside length); ts is the wall thickness of steel tubes; L is the length of samples.

Table 1: Sample list

Serial number	Sample number	Section type	D(B)×ts×L	fcu
1	CCFT-1	circular	200×2.8×600	69.6
2	CCFT-2		1000×2.8×600	69.6
1	CCFT-1	square	200×2.8×600	69.6
2	CCFT-2		1000×2.8×600	69.6

When processing the circular CFST samples, hollow steel tubes are first processed according to the required length and outer diameter to guarantee that the two ends of the steel tubes are flattened. Two circular steel plates with a thickness of 3 mm are machined as cover plates for each sample. The cover plates are first welded to one end of the empty steel tube, and the other end is welded after concrete is cast and the volume is relatively stable (1 day). The cover plates and hollow steel tubes are geometrically centered. The steel tubes of the square CFST samples are made by welding four steel plates. Two steel plates with a thickness of 3 mm are processed as cover plates for each sample.

The average thickness of steel plate is ts = 2.8mm; its yield limit is fy = 340MPa; tensile strength is fu = 439.6MPa; elastic modulus is Es = 2.07 × 105MPa; Poisson's ratio is sμ = 0.267.

Fly ash self-compaction high-performance concrete is adopted, and its materials are as follows:

1. Cement: grade-42.5 normal portland cement produced by Fujian Shunchang Cement Plant;
2. Gravel: Fujian Minhou granite gravel with a maximum particle size of 30mm;
3. Sand: Fujian Minjiang medium sand with a fineness modulus of 2.6;
4. Fine mineral admixture: Class I fly ash of Xiamen Songyu Power Plant;
5. Additive: UNF-5 retarding superplasticizer with the amount of admixture of 0.8% of the total amount of cementitious materials.

Concrete is stirred by mixers. The average internal temperature of concrete is 29.7°C; the slump of the freshly mixed concrete is 280 mm; the horizontal spreading is 670 mm; the time of traversing the 800mm L-type flowmeter is 14s; the flow rate is 57 mm/s; the final flow distance of the L-type flowmeter is 1070mm. The test samples are placed in the laboratory for natural conservation after being cast. The concrete block samples consist of three 150×150×150mm cubic block samples and three 150×150×300mm prismoid block samples, all of which are moulded and maintained under the same conditions as the samples. The test methods are conducted based on the national standard of *Standard for Test Method of Mechanical Properties on Ordinary Concrete (GB/T50081-2002).* The measured 28-day cubic compressive strength of concrete fcu=69.6MPa and elastic modulus Ec=3.71×104MPa.

3.2 Experimental apparatus and experimental methods

The section of the four CFST samples in this temperature field test are symmetrical planes, so it is advisable to measure 1/4 section. The layout of the monitoring points in the temperature field is demonstrated in Figure 1, 2, 3 and 4.
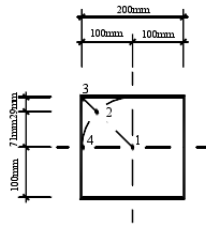
Figure 1: Sketch map of cross section of Sample SCFT-1
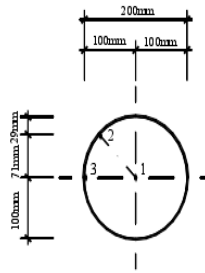

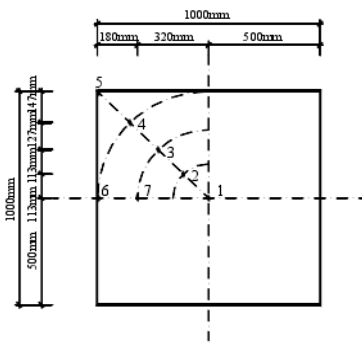Figure 2: Sketch map of cross section of Sample CCFT-1
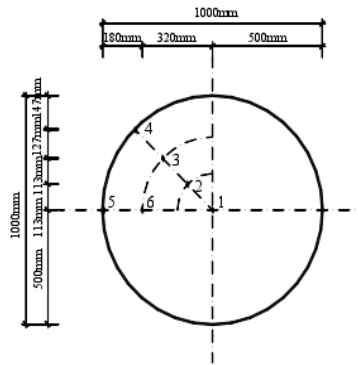

Figure 3: Sketch map of cross section of Sample SCFT-2

Figure 4: Sketch map of cross section of Sample CCFT-2

3.3 Data acquisition pre-operation and data acquisition

The copper-constantan thermocouple used in this experiment is 2×φ0.5mm. The experimental data was collected by a T-type thermocouple in the SI 35951A board of the IMP data acquisition system. The time interval between adjacent sampling points was 1 minute. Prior to experiment, the ends of the two thermodes were connected to each other as the temperature measurement points, and soldering tin was applied externally to form a closed loop with the data acquisition system. The thermocouples at all measuring points were located on the central section of the samples.

The temperature test lasts 45 days. At the beginning of the experiment, the amount of hydration heat released by cement was enormous and the temperature of the test samples changed drastically. Therefore, during the first 7 days, data was collected continuously for 24 hours; from the 7-th day to the 28-th day, data was collected twice a day; from the 28-th day to the 45-th day, data was collected every three days. The time interval for data collection is larger and larger.

4. Results and analysis
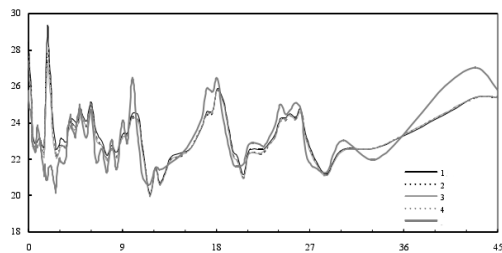
4.1 Experimental results and analysis

Figure 5: Measured temperature curve of each test point of sample section

Figure 5 illustrates the measured curve of the cross-section temperatures of four CFST samples in the cement hydration stage. The average storage temperature of the sample concrete is 29.7°C.

The temperature at each measurement point of the sample section first drops, then continues to rise to its peak value, and falls sharply until it approaches the indoor atmospheric temperature. This is mainly because the formulated high-performance concrete incorporates the retarding superplasticizer, which effectively slows down the early hydration of cement. As a result, the heat released in the hydration of cement does not begin to rapidly intensify until 32 hours after concrete casting. At this time, the rate of hydration exceeds the rate of heat dissipation, and the temperature of the core concrete shows a sharp upward trend. The time when the hydration rate and the rate of heat dissipation reach equilibrium is the peak time.

As indicated by Figure 5, in the initial stage of concrete casting, the distribution of the temperature field of the sample section demonstrates a pattern of inside high and outside low. The large temperature difference between the center and the outer edge of the section steps up with the increase of the section dimension. In terms of Sample SCFT-1 and Sample SCFT-2, their maximum temperature differences between the center and the outer edge of the section are 2.2°C and 14.2°C; in case of Sample CCFT-1 and Sample CCFT-2, the maximum temperature differences are 0.9°C and 7.4°C respectively. Therefore, when the cross-sectional dimensions (diameter of section for circular CFST and side length of section for square CFST) are the same, the maximum temperature difference between the center and the outer edge of the square CFST samples is larger than that of the circular CFST samples. This is mainly due to the fact that, with the same cross-sectional dimensions, the volume of square CFST samples is larger and their heat of hydration is stronger than that of circular CFST samples. In the early stage of concrete casting, the temperature of the sample cross-section is significantly higher than the indoor air temperature, whose temperature difference raises with the increase of the cross-sectional dimensions. For Sample SCFT-1, the maximum temperature difference between its section center and the indoor atmosphere is 8.4°C, while that of Sample SCFT-2 is 26.9°C; for Sample CCFT-1 and Sample CCFT-2, the maximum temperature differences are 7.1°C and 20.4°C respectively.

4.2 Finite element analysis of temperature field

In the stage of cement hydration, the temperature distribution of the cross-section of the CFST member changes with time. In view of this, the heat conduction problem of the CFST structure is nonlinear transient, whose differential equation of heat conduction is a nonlinear parabolic partial differential equation. To solve such differential equations, a solution combining the finite element method and the finite difference method is used in most cases. In other words, the finite element mesh is used in the spatial domain and the finite difference mesh is adopted in the time domain. This method makes full use of the advantages of the finite element method in spatial domain partitioning and the advantages of the finite difference method in time advancement.

4.3 Thermal performance of steel and concrete

The thermal performance parameters of steel mainly include thermal conductivity s_k, specific heat s_c, and volume-weight s_ρ. In general, the heat conductivity coefficient of steel decreases with the increasing temperature, but when the temperature exceeds a certain limit, the heat conductivity coefficient becomes almost constant. The expression for the steel heat conductivity coefficient, s_k, is: 1868.448022.0sTk×+−=k J/(m·h·°C)0°C≤T≤900°C, where T is the temperature (°C).

4.4 Analysis and summary

First, this paper conducts a theoretical analysis on the creep characteristics of the normal concrete and the core concrete in CFST, explains their differences, collects the current typical calculation models for the creep of concrete at home and abroad, applies numerical methods to check calculations of the experimental data of the axially loaded and eccentrically loaded CFST under the action of long-term loading, and explores the feasibility of applying the calculation models for the creep of concrete to predict the deformation of the core concrete in CFST under long-term loading.

Based on the above analysis results, the following conclusions can be initially drawn:

1. Compared with the normal concrete, the core concrete in CFST holds a largely different creep, which is embodied in the working environment and the stress process of the core concrete.

2. Long-term loading ratio and steel ratio exert an enormous influence on the deformation of the 7core concrete in CFST under long-term loading. The time of deformation becoming stable is prolonged as the long-term load ratio increases, and the deformation expands with the long-term load ratio. The greater the steel ratio is, the smaller the deformation amount is.

4. Conclusion

In the early stage of concrete casting, the temperature field distribution of the section of the CFST samples presents a regular pattern of inside high and outside low, and the temperature difference between the center and the outer edge of the section increases with the increase of section dimensions. The section dimensions have a great influence on the shrinkage deformation of the core concrete in CFST. In other words, as the section dimensions expand, the shrinkage deformation of the core concrete is downsized. The reasonable determination of the cross-section temperature field of CFST members at the stage of cement hydration and the calculation models for the shrinkage and creep of the core concrete is of vital significance to designing a more scientific CFST structure.

The changes in the form of cross-section exert certain influence on the shrinkage deformation of the core concrete in CFST. In the early development stage of deformation, the shrinkage deformation of circular CFST is slightly smaller than that of square CFST, and the former one gradually exceeds the latter as time grows. Moreover, the experimental results also indicate that the greater the steel ratio is, the smaller the amount of deformation is. On the whole, this effective study can prevent the heat of hydration.

References

Cao G., Hu J., Zhang K., He M., 2015, Simple model of creep coefficient for expansive concrete filled steel tube, Journal of Building Structures, 36(6), 151-157, DOI: 10.14006/j.jzjgxb.2015.06.019

Chew K.H., Klemeš J.J., Alwi S.R.W., Abdul Manan Z., 2013, Industrial implementation issues of Total Site Heat Integration, Applied Thermal Engineering, 61(1), 17-25, DOI: 10.1016/j.applthermaleng.2013.03.014

Huang Y., Xiao J., Shen L., 2016, Damage assessment for seismic response of recycled concrete filled steel tube columns, Earthquake Engineering & Engineering Vibration, 15(3), 607-616, DOI: 10.1007/s11803-016-0347-8

Kang H.Z., Yao L., Song X.M., Ye Y.H., 2012, Experimental Study on Compressive Bearing Capacity of High Strength Concrete-Filled Steel Tube Composite Columns, Advanced Materials Research, 368-373, 410-414, DOI: 10.4028/www.scientific.net/AMR.368-373.410

Klemeš J.J., 2013, Handbook of Process Integration (PI): Minimisation of Energy and Water Use, Waste and Emissions, Woodhead Publishing Limited, Cambridge, UK.

Klemeš J.J., Varbanov P., Lam H.L., 2009, Water Footprint, water recycling and Food Industry Supply Chain, Chapter In: K Waldron, Waste management and co-product recovery in food processing, 2, Woodhead Publishing Limited, Cambridge, UK, 134-168.

Krishan A.L., Chernyshova E.P., Sabirov R.R., 2016, Calculating the Strength of Concrete Filled Steel Tube Columns of Solid and Ring Cross-section, Procedia Engineering, 150, 1878-1884, DOI: 10.1016/j.proeng.2016.07.186

Lu Y., Li N., Li S., 2014, Behavior of FRP-Confined Concrete-Filled Steel Tube Columns, Polymers, 6(5), 1333-1349, DOI: 10.3390/polym6051333

Montejo L.A., 2012, Seismic Performance Evaluation of Reinforced Concrete-Filled Steel Tube Pile/Column Bridge Bents, Journal of Earthquake Engineering, 16(3), 401-424, DOI: 10.1080/13632469.2011.614678

Raissi K., 1994, Total site integration, PhD Thesis, University of Manchester Institute of Science and Technology, Manchester, UK.

US DoE, 2016, Steam Turbines, US Department of Energy <energy.gov/sites/prod/files/2016/09/f33/CHP-Steam%20Turbine.pdf> accessed 24.07.2017.

Yuan H., Dang J., Aoki T., 2014, Behavior of partially concrete-filled steel tube bridge piers under bi-directional seismic excitations, Journal of Constructional Steel Research, 93(2), 44-54, DOI: 10.1016/j.jcsr.2013.10.022Get rights and content

Zhou X.J., Mou T.M., Fan B.K., Ding Q.J., 2012, Mechanical Properties and Volume Deformation of Steel Fiber Reinforced Micro-Expansive Concrete Filled Steel Tube, Applied Mechanics & Materials, 204-208, 4083-4087, DOI: 10.4028/www.scientific.net/AMM.204-208.4083